3D FINITE ELEMENT MODELING OF MSD-CRACKED STRUCTURAL JOINTS

J. Edward Ingram
Technical Fellow
Lockheed Martin Aeronautics

Young S. Kwon
Staff Engineer
Lockheed Martin Aeronautics

Major Scott A. Fawaz
Chief, Structural Mechanics Division
Department of Engineering Mechanics
United States Air Force Academy

Abstract
Published research has shown that engineering models for crack link-up, based on plastic zone touch criteria, can be good predictors of residual strength. Much of the work that demonstrated the feasibility of this concept was based on analysis and tests of open hole specimens, for which *K* calculations are relatively straightforward. This paper presents the results of an effort to accurately model the Multiple-Site Damage (MSD)-cracked joint configurations, and develop the stress intensity solutions needed to apply the engineering link-up model to structural joints.

Existing stress intensity (*K*) solutions for MSD cracked joints, such as fuselage skin splices and wing chordwise joints, typically do not account for fastener force redistribution as a lead crack extends from one fastener hole to the next, and from MSD cracks at fastener holes. Without this load redistribution information, the normal procedure, after first ligament (one hole spacing) failure, has been to calculate *K* as if the crack were extending through open holes.

Detailed finite element models, utilizing nonlinear solids and interface (contact) elements were developed to calculate the fastener forces and stress intensities in bolted joints containing multiple cracks. Three basic configurations of the parameterized models were created: two-row and three-row single shear joints, and two-row double shear joints. A 3D Virtual Crack Closure Technique (3DVCCT) was used to calculate stress intensity at the lead and MSD cracks.

This paper discusses the development of the 3D models, studies conducted to verify their accuracy, and the parametric analyses of the various joint and crack configurations. A description of how the 3d models were used to update the engineering link-up method is also presented. Comparisons are made between calculated link-up stress levels from the updated engineering method and results from wide panel joint tests containing lead and MSD cracks.

Development of the Parameterized Detail Models
A Lockheed Martin finite element code, DIAL, was selected to model three basic types of structural joint configurations, 2-row lap (single shear), 3-row lap and 2-row butt (double shear). This set of joint configurations allowed us to simulate a number of joint test configurations and extend the results of the analysis to the realistic WFD-susceptible aircraft configurations. Any of a number of FEM codes possess the nonlinear (parabolic) solid elements and nonlinear solution process (modified Newton-Raphson) capabilities that were judged to be needed for this task. The fact that DIAL included these capabilities, as well as the parameterized input method and a convenient interface element to simulate bearing surface contact, led to its selection.

For each model configuration, all of the components of the joint (splice plates and fasteners) were represented using 20 node parabolic solid elements. Wherever contact behavior is simulated, an eight node, two-dimensional interface element is used. The 20 node solid elements have eight nodes on each face (corner and midside nodes); and, as used in these models, match perfectly with the interface elements. The interface elements were given very high compression-normal stiffness values, and zero shear or sliding stiffness, (and zero tension).

One of the primary goals for these models was to be able to run a sufficient number of lead crack and MSD crack combinations to develop trends from which an engineering model could be derived. Thus, the crack configurations (sizes and shapes) were among the variables built into the parameterized input. To a large extent, the parameterization proved successful in permitting numerous solutions. However, it was not possible to build unlimited variability of the crack configurations into each model. Within each joint type, it was necessary to create sub-models for each number of ligaments (between fastener holes) in the lead crack. In other words, a lead crack, which consisted of one failed ligament plus an emerging crack out of the adjacent two holes was one sub-model. A lead crack with three failed ligaments was another sub-model, and so on. Figure 1 shows a plot of a typical model. In this example, the model is a 2-row lap joint, with a lead crack encompassing one failed ligament. The model is symmetric about the lower right edge.

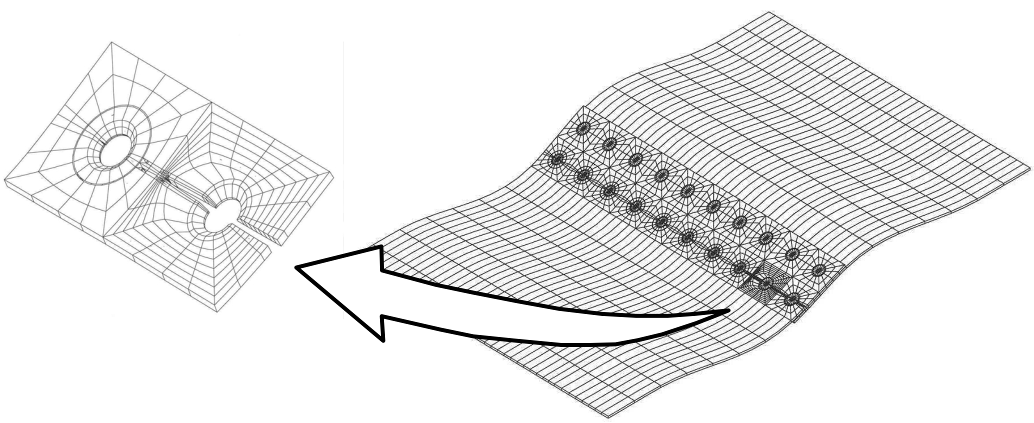

Figure 1: 2-Row DIAL Lap Joint Model with One Failed Ligament

The local region near the crack front is illustrated in Figure 2. As the figure shows, the parametric DIAL input was configured to produce a very refined mesh ahead of, and behind the crack.

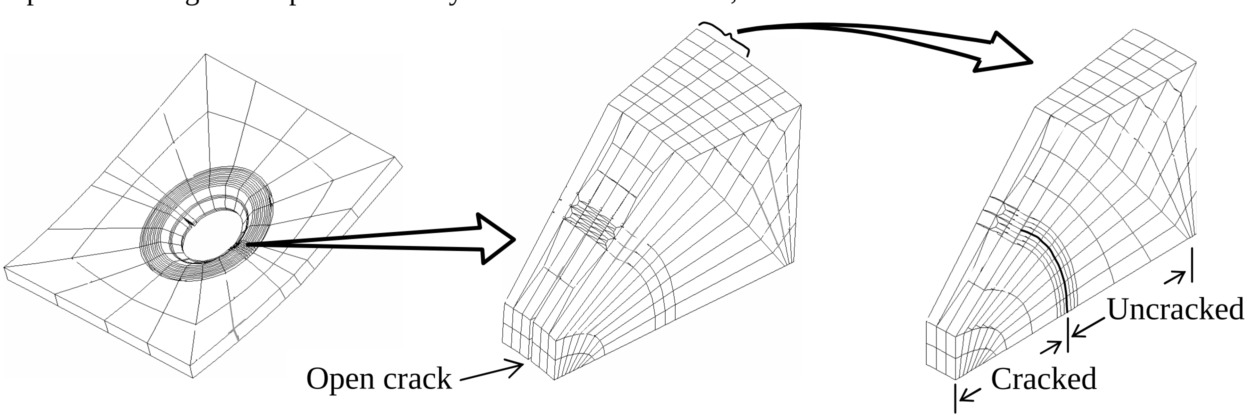

Figure 2: DIAL 3D Model Mesh Near the Crack Front

Note the series of narrow, constant thickness elements on either side of the crack front. This region, referred to as the “crack band”, has sufficient refinement and element regularity (consistent spacing and absence of skewness) to accurately calculate the nodal forces and displacements in this area where the stress gradient is high. Several types of studies were conducted to establish the “rules” that would be incorporated into the parametric input to maintain good mesh in the crack band for all crack shapes. Well known stress intensity solutions for part-through cracks from open holes and from single-edge notched tension (SENT) specimens were available from Zhao et. al. [1,2]. DIAL models of the cracked SENT and open hole configurations were created and studied for the effect of mesh imperfection on accuracy.

A 3D Virtual Crack Closure Technique (3DVCCT) was used to calculate the stress intensity along the lead crack and MSD crack fronts. This version of the virtual crack closure method uses forces at nodes “ahead of” the crack front (the un-cracked region), and displacements “behind” the crack front (in the crack wake) to calculate the strain energy release rate with a single execution of the model. A thorough description of the 3DVCCT method was given by Shivakumar, et. al. [3] and Fawaz [4]. The single execution (as opposed to solving once for forces and again for displacements at the same nodes) was particularly important in this study, as the nonlinear solution of the large (>200,000 degrees of freedom) models required days to complete, and well over 100 variations of the parametric models were run. The requirement for nonlinear solution of the models stemmed from the contact behavior at the bearing surfaces and from the secondary bending due to eccentric load paths. A far-field or remote load corresponding to a stress of 10 ksi was selected as the target load for each run. This value was reasonable from the standpoint of typical operational loading at these types of aircraft joints.

Once the K at each point along the crack front was calculated, the normalized stress intensity, F, for a quarter-elliptical part-through crack is:

$$F = \frac{K}{S\sqrt{\frac{\pi a}{Q}}}$$

Where S is the remote stress, and Q is the crack shape parameter, computed as follows:

$$Q = 1 + 1.464\left(\frac{a}{c}\right)^{1.65} \quad for \quad \frac{a}{c} \leq 1 \qquad and \qquad Q = 1 + 1.464\left(\frac{c}{a}\right)^{1.65} \quad for \quad \frac{a}{c} \geq 1$$

For through-cracks, the normalized stress intensity is:

$$F = \frac{K}{S\sqrt{\pi a}}$$

Figure 3 is typical of one of the comparisons of DIAL model results to the published results. The agreement is generally good, but not perfect. The slight differences are thought to be related to the use of 20 node solids in the DIAL models and 8 node bricks in the solutions from [1] and [2]. There are also differences in the degree of mesh refinement in these models.

Once it was established that the DIAL models with obviously acceptable mesh refinement and regularity agreed with these known solutions, a number of studies were launched to study the effects of various mesh imperfections, such as element skewness, high aspect ratios, and abrupt fine/coarse mesh transitions.

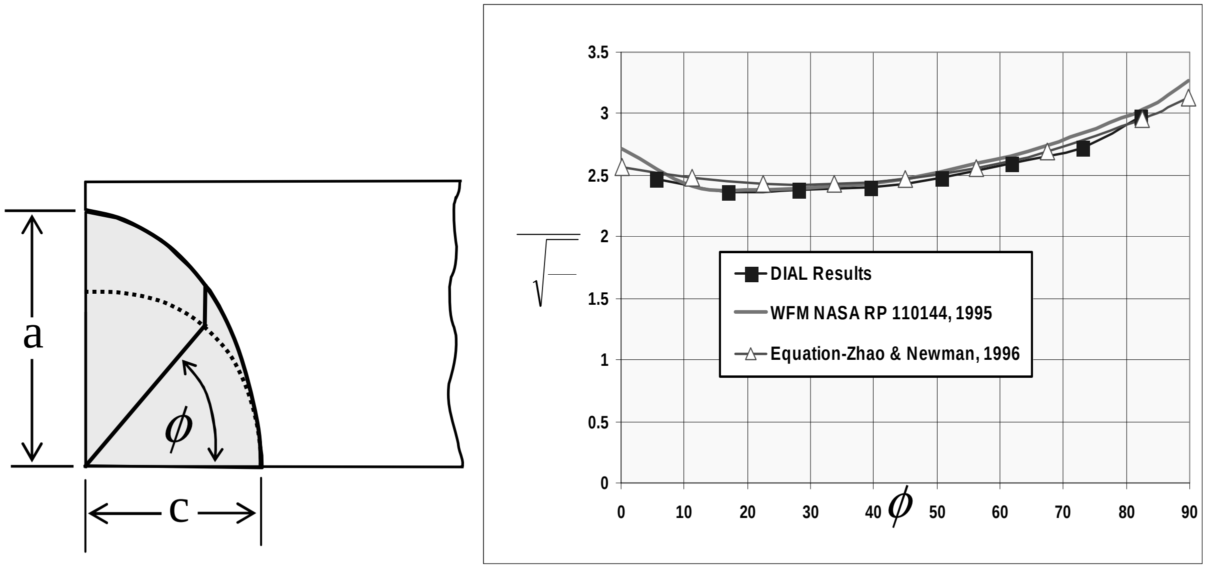

Figure 3: Comparison of DIAL 3D Model Results to Established Solutions for Part-through Cracks at Open Holes

The following mesh rules, regarding the elements in and near the crack band, were derived from these sensitivity studies:

- Three rows of identical solids ahead of and behind the crack front (in the high stress gradient region) are required.
- Element aspect ratios for the 20 node parabolic solids shall not exceed 10 (provided the requirements of 1 are met).
- Element skew (trapezoidal shape) shall not exceed 30 degrees (angles formed by two adjacent element faces should be within 30 degrees of orthogonal).

Parametric Model Solutions

After establishing the mesh rules and incorporating them into the DIAL parametric language, 13 separate model configurations were created. The joint and/or crack configurations that necessitated separate models, included:

- Three joint types: two-row and three-row single shear lap joints, two-row double-shear butt joints
- Three lead crack configurations: one, three and five ligaments failed
- Through and part-through crack shapes
- Separate models for calculating K at the lead crack and at the MSD crack (mesh refinement sufficient for 3DVCCT calculations at one crack per model to reduce model size).

Figure 4 is a graphical representation of the normalized stress intensity solution obtained from a series of 3 model executions. This plot shows F along the crack front for the case of Three ligaments cracked in a two-row single shear splice, and shows the influence of the adjacent MSD crack size. In this case, the lead crack has a local length (measured from the hole) of 0.20 inch and various MSD crack sizes. These results show the expected trend of a nonlinear effect of MSD crack size on the lead crack K. However, the true significance is not in confirming this expectation – the importance is in quantifying this effect with the realistic effects of fastener force redistribution and secondary bending in the joint. Numerous calculations and plots such as the one in Figure 4 were made to create a database of solutions and develop equations that reasonably approximate these model results.

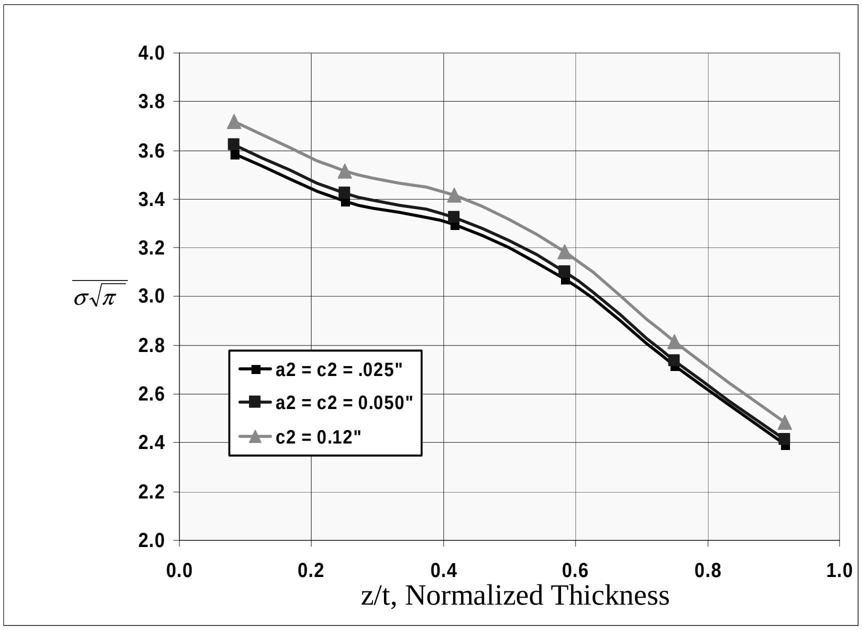

Figure 4: DIAL 3D Model Results for 2-Row Single Shear Joint with Three Ligaments Failed, Local Lead Crack Length = 0.20 inch, and Varying MSD Crack Sizes

Parametric Model Fastener Force Results

One of the primary goals for the 3D model development was to study how the fastener forces redistribute as a function of crack configuration. With this type of information, superposition procedures can be used to develop the engineering approximation equations. Figure 5 shows typical distributions of fastener forces, calculated from three DIAL model solutions, for a 2-row splice with varying lead crack lengths. The fastener forces were determined automatically within the DIAL execution by calculating the component (in the direction of the applied load) of the normal force on each interface element, and summing these components for all interface elements at the fastener/hole combination. The bar chart of Figure 5 shows the expected trend of increasing lead crack length causing reduced local stiffness and reduced fastener forces at each fastener absorbed by the lead crack. The load shedding in the crack path is accompanied by shifting some of the load to fasteners ahead of the lead crack, and some to the un-cracked row.

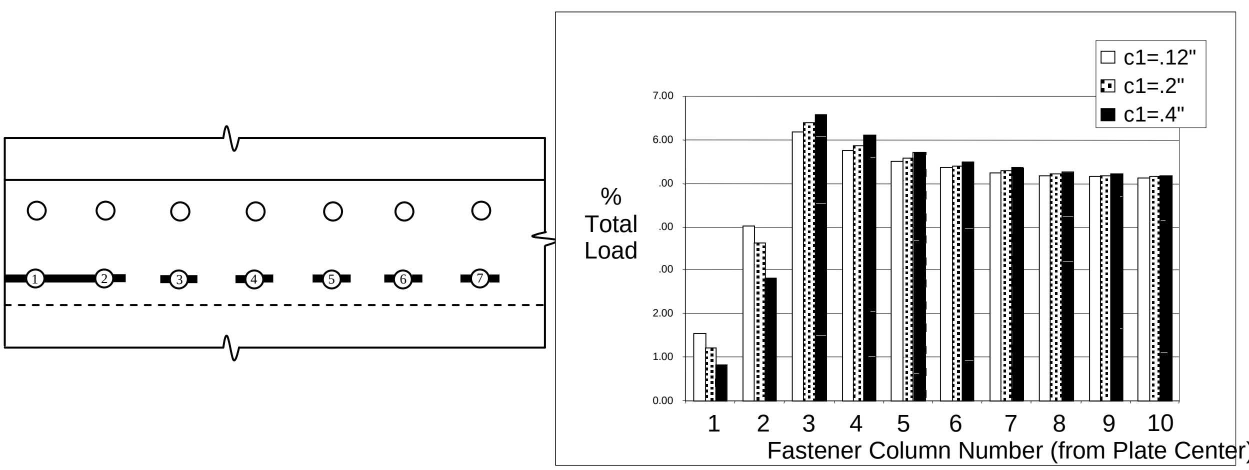

Figure 5: 3D Model Results - Distribution of Fastener Forces in a 2-Row Single Shear Joint with Lead and MSD Cracks

The DIAL-calculated fastener distribution for a 3 row joint is shown in the chart of Figure 6. The chart shows the expected trends:

- The first and third rows develop greater fastener forces (remote from the crack) than the row 2
- The cracked row shows the shedding and peaking behavior observed in the 2-row joint (Figure 5)
- The lead crack in row 3 affects the magnitude of load in the other rows in the region near the crack

Another interesting feature of the force distribution may also be observed - the largest fastener force occurs in row 1 (un-cracked row), at a distance from the panel centerline just greater than the lead crack length.

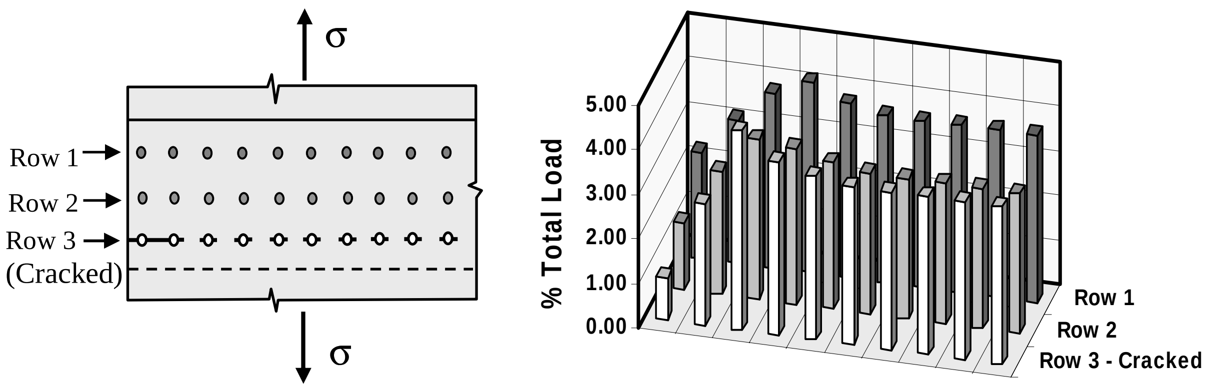

Figure 6: Fastener Forces from a DIAL Model of a 3-Row Joint

The load shedding and peaking behavior shown in Figures 5 and 6 is shown in a different way in Figure 7. In this figure, the changes in several fastener forces are plotted against increasing lead crack length. When the lead crack is small all of the fastener forces tend to be approximately the same magnitude (about 300 lb). As the lead crack lengthens beyond one ligament, the force in fastener 1 (P_{f1} – the open diamonds) exhibits a significant drop - resembling an exponential decay. In this same lead crack range, the other fasteners in the same row (P_{f2}, P_{f3} and P_{f4}) show increasing force. When the lead crack extends through the next ligament, fastener 2 (P_{f2}) shows the same type of exponential drop. This pattern repeats each time the lead crack extends past a fastener hole.

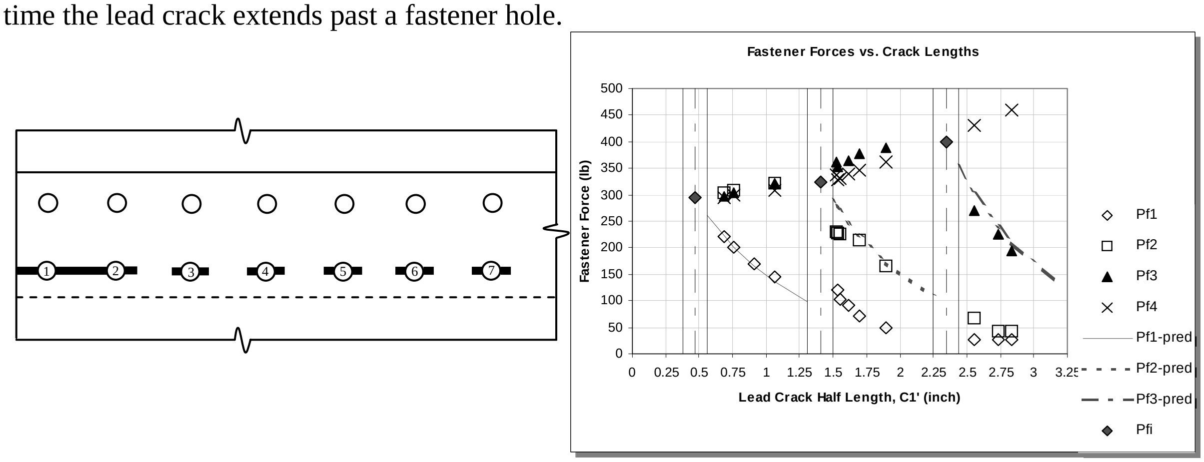

Figure 7: Redistribution of Forces at Several Fasteners as the Lead Crack Extends

The solid, dotted and dot-dash curves in Figure 7 represent an exponential function that was derived to best fit the behavior calculated by the models. Note that each time the decay function repeats for an additional ligament crack, it initiates from a slightly higher force. This beginning point is the "peaking" behavior shown in the earlier bar charts, in which the next higher fastener in the crack path is absorbing the load shed from the cracked fastener holes. The peaking behavior is proportional to the length of the lead crack in a similar way as local stress ahead of a crack tip. The values represented by the solid diamond symbols were calculated using the following equation, which incorporates the square root of the distance to the fastener (x_i) and is then best-fit to the DIAL results using a natural log function.

$$P_f = N_x S(PLT)\sqrt{x_i}\left[-0.118\ln(x_i)+0.915\right]$$

N_x is the uniform far-field load and PLT is the percent load transferred in the critical row. Once the peak value of each fastener force is determined for each ligament, the subsequent force decay is calculated from:

$$P_f(c_1) = P_{next}\ln(-1.3c_1)$$

The previous equations provide the means to quickly calculate (without additional finite element modeling) a fastener force for a given crack configuration. Once the fastener forces are determined, the stress intensity solutions for the lead and MSD cracks can be calculated using superposition of existing solutions. The stress intensity for the fastener forces on the crack flanks are accounted for using a solution from Wu and Carlsson [5] for point forces on crack faces. The stress intensity solution for the MSD cracks at fastener holes ahead of the advancing lead crack is calculated using a Lockheed Martin solution for bearing and bypass stress on a cracked loaded hole. These solutions were incorporated into a code for calculating *K* at the lead crack and at the MSD cracks.

Methodology for Crack Link-up

A number of researchers, including Swift [6] and Broek [7] have proposed a crack link-up method based on a plastic zone touch criteria. The plastic zone touch criteria does not account for the effects of plasticity with quite the same technical rigor as J Integral or T* Integral techniques, but is far simpler and with some modification or tuning is sufficiently accurate. The tuned plastic zone method is sometimes referred to as the engineering link-up model. Broek [7], Smith [8] and Ingram [9] have developed various forms of this engineering model for 2024-T3. Comparisons of the engineering models to test data have shown that it can predict link-up stress levels within approximately 3% to 5% for multiple cracks in open hole or slit-crack specimens. The engineering model relies on calculating *K* at the lead crack and MSD cracks accurately. This is relatively straightforward for open holes or slit-cracks. To use this method in a structural joint requires a method to predict *K* at the loaded holes, which motivated the 3D DIAL model work described earlier.

Comparison to Test Results

The *K* calculations, based on the DIAL model results and the engineering model developed from the open hole and slit-crack tests, were used to calculate link-up stress (far-field stress at the instant of link-up) for two series of tests of MSD-cracked bolted joints. The first joint specimens were tested by the Air Force Research Labs (AFRL) during the FAA/USAF/Boeing Widespread Fatigue Damage Program. The test set-up and results were reported in [10]. These specimens were 48 inch wide 2024-T3 panels with various joint configurations similar to those found on commercial transport aircraft. All of the specimens were tested with anti-buckling guides, which, in addition to preventing crack face buckling, also prevented the natural rotation and secondary bending in the joint due to the eccentric load path. The measured crack link up stress results from these tests and the analysis results from the DIAL-based engineering link-up model are summarized in Table1.

TABLE 1: Summary of AFRL MSD Test Results [11] and Comparison to Calculated Values

Test ID MSD -	**Fast. Spac.** (inch)	**Fast. Dia.** (inch)	**Crack Half-Length** a_{msd} (inch)	a_1 (inch)	$a_{1\text{-local}}$ (inch)	**Ligament Length** (inch)	**Test Event**	**Test Stress** (ksi)	**Calculated 3D Models** (ksi)	**% Error**
1-2125	1.5	5/32	0.05	6.950	0.872	0.422	1st Link-up	14.90	12.11	-18.72
			0.05	7.628	0.050	1.244	Max Load	17.20	18.08	5.10
1-3			0.10	6.950	0.872	0.372	1st Link-up	12.52	11.51	-8.04
			0.10	7.678	0.100	1.144	Max Load	17.42	17.51	0.52
501-2	1.14	3/16	0.05	6.410	0.616	0.286	1st Link-up	13.23	11.41	-13.77
			0.05	6.984	0.050	0.853	Max Load	17.97	16.78	-6.62
501-3			0.10	6.410	0.616	0.236	1st Link-up	11.24	9.76	-13.21
			0.10	7.034	0.100	0.753	Max Load	14.90	15.87	6.50
503-2	1.6	3/16	0.05	7.400	0.906	0.456	1st Link-up	14.29	12.66	-11.41
			0.05	8.144	0.050	1.313	Max Load	18.31	17.39	-5.00
503-3			0.10	7.400	0.906	0.406	1st Link-up	12.24	11.39	-6.98
			0.10	8.194	0.100	1.213	Max Load	16.62	16.46	-0.99
505-2	1.5	5/32	0.05	6.950	0.872	0.422	1st Link-up	15.43	13.03	-15.58
			0.05	7.628	0.050	1.244	Max Load	19.69	18.38	-6.65
505-3			0.10	6.950	0.872	0.372	1st Link-up	13.70	11.70	-14.58
			0.10	7.678	0.100	1.144	Max Load	18.44	17.84	-3.28
									Average Error =	-8.6 %

The average error for all test events in the AFRL series was -8.6%. If only test failures (final link-up or specimen residual strength) are considered, the average error is -4.3%. In general, the analysis under-predicted the test results. The somewhat higher percent error in the analysis of the joint tests as compared to the open hole tests is thought to be due mostly to the secondary bending effects. The DIAL 3D models were not constrained to prevent secondary bending, as they were intended to represent the conditions on the aircraft to the maximum extent possible. The bending stress increases the maximum stress intensity calculated for each crack tip, which reduces the calculated link-up stress.

A second set of joint tests were conducted by Hijazi, et. al. [11] at Wichita State University. These test specimens were 24 inch wide 2024-T3 clad lap joints with three rows of steel neat-fit fasteners. The sheet thickness (0.056 inch), rivet size (3/16 inch) and rivet spacing (1.00 inch) were identical for all specimens. Only the crack lengths were varied. As in the AFRL tests, anti-buckling guides were used. Table 2 summarizes the initial crack lengths installed (by jeweler's saw) in the panels, the measured link-up stress and the calculations from the DIAL-based link-up model. Nine of the 36 tests were conducted with no MSD cracks – lead crack only. The current version of the engineering link-up model is capable of analyzing only cases where a lead crack and MSD cracks are present. Therefore, to simulate the nine tests without MSD, very small MSD cracks (0.001 inch) were assumed in the analysis.

The average error for all 36 analysis-test comparisons was -8.4%. If the zero-MSD specimens are omitted, the average error is -7.7%. As with the AFRL tests, the analysis predicted lower link-up stresses than were measured, and likely for the same reason – the secondary bending effects. Additional tests are planned in which secondary bending will be allowed, and the accuracy of the link-up methodology will be re-examined. Until this data is available, the approach will be to continue with the current model, as it is better to under-predict than over-predict.

TABLE 2: Summary of WSU MSD Test Results [11] and Comparison to Calculated Values

Test ID MSD -	**Crack Half-Length** a_{msd} (inch)	a_1 (inch)	$a_{1\text{-local}}$ (inch)	**Ligament Length** (inch)	**Test Stress** (ksi)	**Calculated 3D Models** (ksi)	**% Error**
1	0.00	4.194	0.10	0.713	20.91	17.477	*-16.42*
2	0.05	4.194	0.10	0.663	18.38	15.698	-14.59
3	0.10	4.194	0.10	0.613	16.79	15.042	-10.41
4	0.00	4.244	0.15	0.663	20.02	16.983	*-15.17*
5	0.05	4.244	0.15	0.613	18.38	15.158	-17.53
6	0.10	4.244	0.15	0.563	16.44	14.481	-11.92
7	0.15	4.244	0.15	0.512	15.45	13.939	-9.78
8	0.00	4.294	0.20	0.613	19.85	16.621	*-16.27*
9	0.05	4.294	0.20	0.563	17.38	14.721	-15.30
10	0.10	4.294	0.20	0.513	16.47	14.012	-14.92
11	0.15	4.294	0.20	0.462	15.34	13.437	-12.41
12	0.20	4.294	0.20	0.413	14.72	12.66	-13.99
13	0.00	5.194	0.10	0.713	17.27	15.473	*-10.41*
14	0.05	5.194	0.10	0.663	15.56	13.967	-10.24
15	0.10	5.194	0.10	0.613	14.88	13.408	-9.89
16	0.00	5.244	0.15	0.663	17.17	15.334	*-10.69*
17	0.05	5.244	0.15	0.613	15.36	13.747	-10.50
18	0.10	5.244	0.15	0.563	14.11	13.156	-6.76
19	0.15	5.244	0.15	0.512	13.10	12.679	-3.21
20	0.00	5.294	0.20	0.613	16.71	15.064	*-9.85*
21	0.05	5.294	0.20	0.563	14.82	13.4	-9.58
22	0.10	5.294	0.20	0.513	13.96	12.775	-8.49
23	0.15	5.294	0.20	0.462	12.80	12.263	-4.20
24	0.20	5.294	0.20	0.413	11.88	11.565	-2.65
25	0.00	6.194	0.10	0.713	14.97	14.036	*-6.24*
26	0.05	6.194	0.10	0.663	12.95	12.708	-1.87
27	0.10	6.194	0.10	0.613	12.51	12.214	-2.37
28	0.00	6.244	0.15	0.663	14.78	13.876	*-6.12*
29	0.05	6.244	0.15	0.613	12.74	12.392	-2.73
30	0.10	6.244	0.15	0.563	11.79	11.871	0.69
31	0.15	6.244	0.15	0.512	10.88	11.449	5.23
32	0.00	6.294	0.20	0.613	14.24	13.552	*-4.83*
33	0.05	6.294	0.20	0.563	12.25	12.092	-1.29
34	0.10	6.294	0.20	0.513	11.57	11.538	-0.28
35	0.15	6.294	0.20	0.462	10.75	11.08	3.07
36	0.20	6.294	0.20	0.413	10.04	10.45	4.08
						Average Error =	-8.4%

The comparison of test and analysis results is shown for both series in Figure 8. Note that the WSU tests seem to exhibit a trend of good agreement when the measured and calculated link-up stresses are in the

10.0 ksi range, and consistently decreasing agreement at higher stress levels. The AFRL tests, while showing approximately the same average error, have no such discernable trend with magnitude of link-up stress.

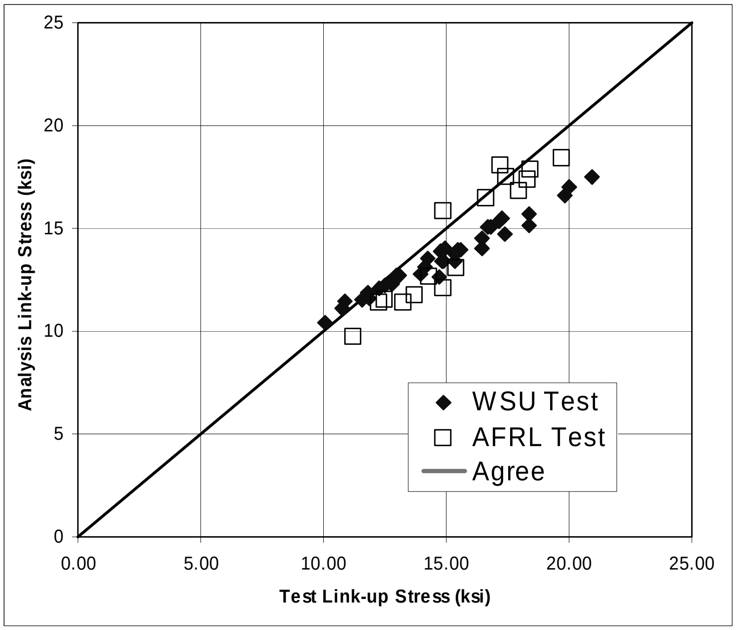

Figure 8 Comparison of Analysis and Test Results for AFRL and WSU Link-up Tests

At this time, no explanation for the trend of the WSU tests has been found. It is obvious that an additional correction factor, or a re-calculation of the link-up model specifically for the WSU tests would significantly reduce the percent error. However, until the physical reason(s) for the differences observed in Figure 8 is determined, no such effort could be justified.

Conclusion

Because no test data have yet been developed which replicate or approximate the secondary bending effects which are expected to occur in real aircraft joints, there is no reason to believe at the present time that the engineering model is not sufficiently accurate for use in residual strength assessments of multiple site damage. Additional limited testing is planned to verify the methods described here for 7075-T6 alloy. These specimens will be tested without anti-buckling guides.

References

(1) Zhao, W., Newman, J. C., Jr., Sutton, M. A., Wu, X. R. and Shivakumar, K. N.,“Analysis of Corner Cracks at a Hole by a 3-D Weight Function Method with Stresses from Finite Element Method,” *NASA TM-110144*, July 1995.

(2) Zhao, W., and Newman, J. C., Jr., “Modification of Stress Intensity Factor Equation for Corner Crack from a Hole Under Remote Bending,” April 1996.

(3) Shivakumar, K. N., Tan, P.W., and Newman, J.C., Jr., “A Virtual Crack Closure Technique for Calculating Stress Intensity Factors for Cracked Three Dimensional Bodies”, *International Journal of Fracture* 36: R43-R50, 1988.

(4) Fawaz, S. A., “Fatigue Crack Growth in Riveted Joints,” Ph.D. Dissertation, Delft University Press, 1997.

(5) Wu, X. R., and Carlsson, A. J., “Weight Functions and Stress Intensity Factor Solutions”, Pergamon Press, 1991.

(6) Swift, T., “Widespread Fatigue Damage Monitoring Issues and Concerns,” *The 5th International Conference on Structural Airworthiness of New and Aging Aircraft*, June 1993.

(7) Broek, D., “The Effects of Multi-Site Damage on the Arrest Capability of Aircraft Fuselage Structures,” FractuResearch TR 9302, June, 1993.

(8) Smith, B., Movak, A., Saville, P., Myose, R., and Horn, W., “Improved Engineering Methods for Determining the Critical Strengths of Aluminum Panels with Multiple Site Damage in Aging Aircraft,” Proceedings of *the 2nd Annual NASA/FAA/DOD Conference on Aging Aircraft*, Williamsburg, VA., Aug. 31-Sept. 3, 1998.

(9) Ingram, J. E., Y. S. Kwon, K. J. Duffié and W. D. Irby, “Residual Strength Analysis of Aircraft Skin Splices with Multiple Site Damage,” Proceedings of *the 2nd Annual NASA/FAA/DOD Conference on Aging Aircraft*, Williamsburg, VA., Aug. 31-Sept. 3, 1998.

(10) Shrage, D. B., “Multiple Site Damage in Flat Panel Testing,” Final Report for Period of 13 May 1999 – 08 December 1999, AFRL-VA-WP-TR-2001-3005, October 2000.

(11) Hijazi, Ala L., Smith, Bert L., and Lacy, Thomas E., “Residual Strength of Bolted Lap Joint Panels with Multiple Site Damage,” *AIAA Journal of Aircraft*, 2002.